



## Connection of a Steel Column Base Plate: Mechanical Behavior and Stiffening Effects

Benyelles Chemseddine Mehdi <sup>1\*</sup>, Nadir Boumechra <sup>1</sup> , Abdelghani Missoum <sup>1</sup>,  
Abdelhamid Bouchair <sup>2</sup> 

<sup>1</sup> *EOLE, Laboratoire Eau et Ouvrages dans Leur Environnement, Département de Génie civil, Faculté de Technologie, Université de Tlemcen, Algeria.*

<sup>2</sup> *Clermont Auvergne INP, CNRS, Institut Pascal, Université Clermont Auvergne, F-63000 Clermont-Ferrand, France.*

Received 19 June 2022; Revised 21 August 2022; Accepted 26 August 2022; Published 01 September 2022

### Abstract

This paper investigates the behaviour of a steel column base connection subjected to a bending moment and compressive axial force. The behaviour of this connection is quite complex due to the number of components, such as the base plate, anchor rods, and stiffeners, to be considered in the numerical models. Moreover, a nonlinear three-dimensional finite element model was used to simulate the column base connection. This model can be used to analyze the moment-rotation relationship for the connection through the validation of numerical modeling with those given by the experimental test results and compared with the analytical model based on the components method of Eurocode 3. It was shown that in addition to the stiffness and bending resistance of the column base connection, other mechanical parameters, such as moment-rotation shape, stress distribution, and prying actions, can be significantly influenced by changing the properties of the components. It has been demonstrated that the anchor rod is not only affected by the axial force but also by a local moment that is not taken into consideration by the analytical model of Eurocode3. An extensive parametric study on stiffeners showed very interesting effects obtained by adding the welded stiffeners to the column base connections.

*Keywords:* Column Base; Base Plate; Stiffness; Prying Actions; Anchor Rod; Stiffener, Eurocode 3.

## 1. Introduction

Column base connections, which are quite popular in steel structures, often consist of a plate welded to the steel profile and bolted to the foundation using anchor rods. They generally transmit normal forces and bending moments to the foundations. It is worth emphasizing that the flexibility of the plate, on the one hand, and the stress concentration in the column-plate connection zone, on the other hand, both generate a variable concentration of pressure under the plate [1]. The column base connection is the final link in a chain that transfers the loads between a steel structure and its foundations. Thus, it is crucial that these connections need to be designed to safely transfer these loads [2]. The column base plate (CBP) connection is one of the most safety-critical components of steel structures since it transfers the vertical forces, the shear forces, and the bending moments from the structure to the foundation [3, 4]. The column base consists of a set of elementary components whose strength and stiffness should be defined and designed in accordance with Eurocode 3 (EN1993-1-8) [5]. Over the past few years, several experimental and numerical studies have been carried out in order to better understand the global behaviour of this connection (axial resistance, bending resistance, bending stiffness) [6, 7].

\* Corresponding author: [chemsoubenelles@gmail.com](mailto:chemsoubenelles@gmail.com)

 <http://dx.doi.org/10.28991/CEJ-2022-08-09-02>



© 2022 by the authors. Licensee C.E.J, Tehran, Iran. This article is an open access article distributed under the terms and conditions of the Creative Commons Attribution (CC-BY) license (<http://creativecommons.org/licenses/by/4.0/>).

It is well acknowledged that the column base connections are very important and have a significant influence on the response of the structure. However, little research work has been carried out on this element compared to that which has been devoted to rigid and semi-rigid beam-to-column and beam-to-beam connections [8]. It has been revealed that predicting the behavior of column bases, such as the moment-rotation relationship, is more difficult and more complex than that of column-beam connections, because several factors are involved in this relationship. These factors include the column stiffness, the dimensions and flexibility of the base plate, the number and position of the anchor rods on the plate, the concrete foundation, and the effect of the contact between the steel plate and the concrete foundation [9].

A common column base consists of several components, like the column cross-section, base plate, stiffeners, anchor rods, concrete foundation, and shear-lug. Each of these components affects the connection's capacity to withstand the axial force, shear force, and bending moment [10]. Some researchers have tried to describe the interactions between the bending moment and the axial forces as well as the effects on some aspects of column base rotational response. Moreover, experimental studies previously carried out have made it possible to develop methods for calculating the bending resistance of column bases [11-16]. Other studies have also been conducted for the purpose of evaluating the rotational stiffness of column bases [17-21]. It should be pointed out that column bases mainly deform when loaded through normal forces, shear forces, and bending moments. Note that, theoretically, the rotational behavior of column bases can generally be idealized by considering a hinge or a stiff connection. Nevertheless, in the majority of cases, their rotational response is an intermediate case between these two situations. In this case, the column bases are considered semi-rigid [22].

Furthermore, a number of theoretical and experimental studies have been carried out on column base connections by Jaspert & Vandegans [22] that succeeded in highlighting the fact that the main modes of column base failure are due to the fracture of the anchor rods, deformation of the base plate, and crushing of concrete. Hon and Melchers [23] investigated the effects of some parameters, such as the base plate thickness and anchor rod size. They suggested that the stiffness of the column base increases significantly when the base plate thickness and anchor rod diameter increase. Ermopoulos and Stamatopoulos [24] proposed a simple analytical formula to describe the relationship between the moment and rotation of the column base.

Otherwise, several experimental studies have been carried out on column bases. The findings revealed that typical failure modes under cyclic loading include rod failure, base plate failure, combined failure of rod and base plate, and column buckling failure [25]. It should be noted that the effective length of the anchor rod is one of the most important parameters for determining stiffness. This effective length can be estimated as equal to 8 times the diameter of the anchor rod [26]. In addition, other experimental and numerical studies have indicated that a rigid column base with 4 anchor rods has a mechanical behavior characterized by the deformation of the base plate in the tension zone and the concrete crushing in the compression zone of the connection [27]. Delhomme et al. [28] performed experimental studies on connections with anchor rods and plates embedded in concrete. The anchor rods were prestressed in order to reduce the fatigue effect. The results showed that concrete does not crack around the anchor plate as long as the prestressing force is less than 50% of the elastic limit of the anchor rod. Similarly, Zhao et al. [29] conducted experimental studies on prestressed anchor rods embedded in rock and successfully demonstrated that prestressing plays an important role in shear strength. Based on a nonlinear finite element model of the column base, Razzaghi & Khoshtakht [30] conducted a study to examine the connection behaviour and identify the effects of different components, such as the base plate, anchor rods, and stiffeners. It was also demonstrated that in addition to column base stiffness, the moment-rotation relationship and the overall stress distribution can be significantly influenced by the characteristics of the basic components. The exposed and embedded base plate connection has been studied by Falborski et al. [31], obtaining that rotational fixity of a column base plate in steel moment resisting frames strongly influences their seismic response. However, stiffened base plates were not considered in this investigation.

The current study aims to assess the effects of some of the most important components of column base connections such as the base plate, anchor rod and stiffeners. A nonlinear three-dimensional finite element model is used to simulate the behaviour of the connection. A bending moment and compressive axial force with prestressing in the anchor rods were applied of the column base plate connection, in order to validate the numerical model by comparison with the experimental results. A detailed study was made on different components of the column base plate. Thus, the analysis concerned the deformation of the base plate, the rotational stiffness of the connection, the failure modes, the prying effect, as well as the forces and the stresses in the anchor rods. The obtained failure modes were then compared with those defined by the analytical models of Eurocode 3. In addition to the previous mechanical parameters, the influence of the stiffeners (position, geometry) on the behaviour of the column base plate was evaluated.

## 2. Research Methodology

This study aims to perform detailed analysis of the behavior of the column base plate considering several parameters such as the base plate, the anchor rods and the stiffeners. It is based on a numerical model validated by comparison with experimental results and used to perform a parametric study. The numerical results, considering a

bending moment and a compression axial force, are used to evaluate the analytical model of Eurocode 3 [5]. The flowchart of the research methodology is shown in Figure 1.

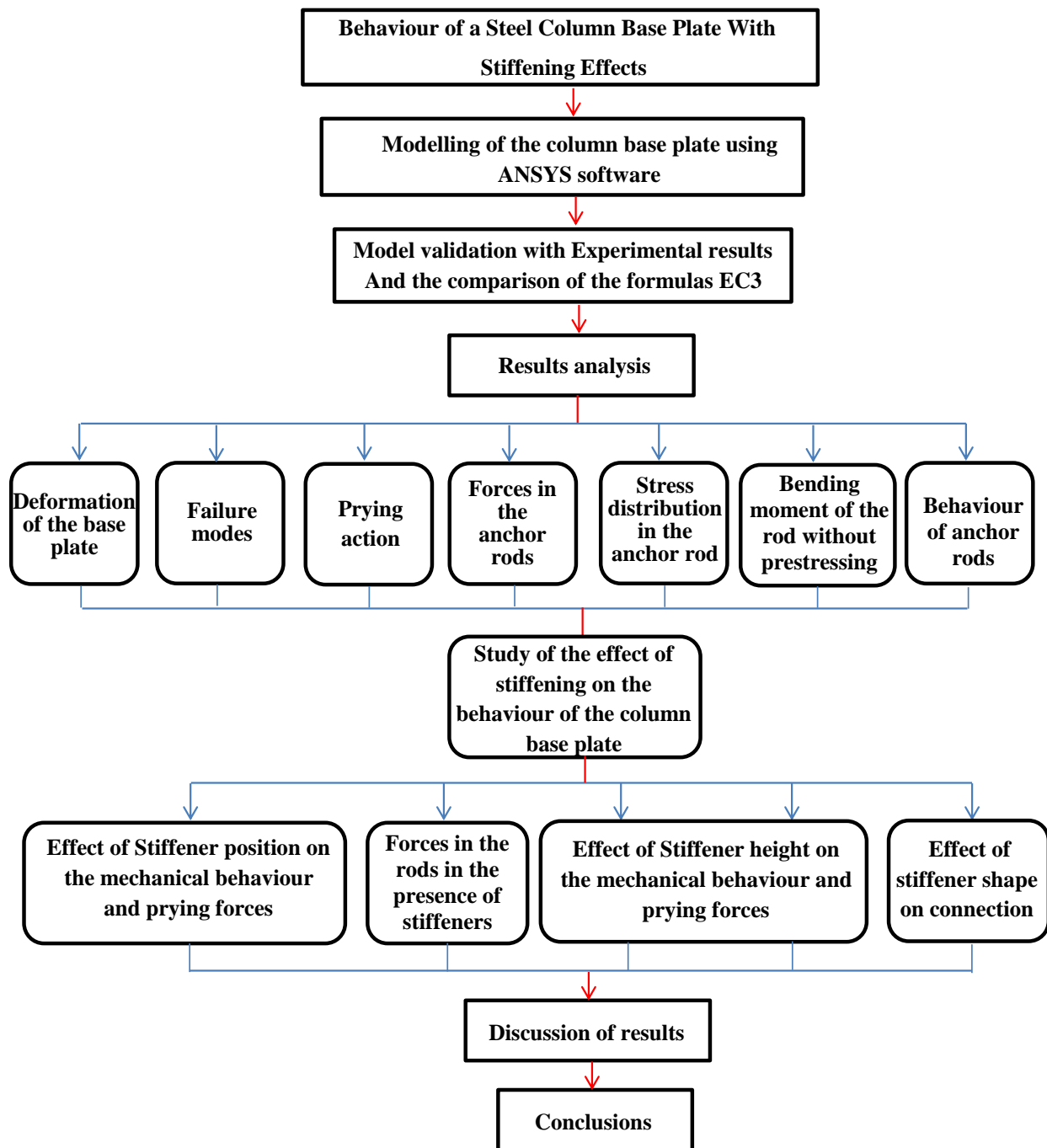


Figure 1. Flowchart of the research methodology

### 3. Validation of the Developed Finite Element Model

#### 3.1. Experimental Testing

The finite element numerical model was validated based on the experimental tests that were carried out at the Materials and Structures Laboratory of the University of Salerno (Italy) [9]. It should be noted that the column was connected to a concrete footing using a base plate and anchor rods. In addition, the concrete footing was fixed to the solid floor of the laboratory by means of a system of four prestressed high-strength bars in order to prevent the rotation of the concrete block, as is clearly illustrated in Figure 2. The vertical axial load  $F_1$  and horizontal load  $F_2$  were applied to the column by means of hydraulic jacks which were placed at the top of the column; the column footing consisted of C20/25 concrete grade. The base plate and concrete footing were connected by means of M20 class 8.8 anchor rods, with a prestressing equal to 80% of the elastic limit.



Figure 2. Column base connection test setup [9]

### 3.2. Geometry of the Tested Connection

The specimen under study consisted of a HEA160 column connected to a concrete footing; its dimensions were (1400×600×600) mm. This column was welded to the base plate with a thickness equal to 15 mm, as shown in Figure 3 and Table 1.

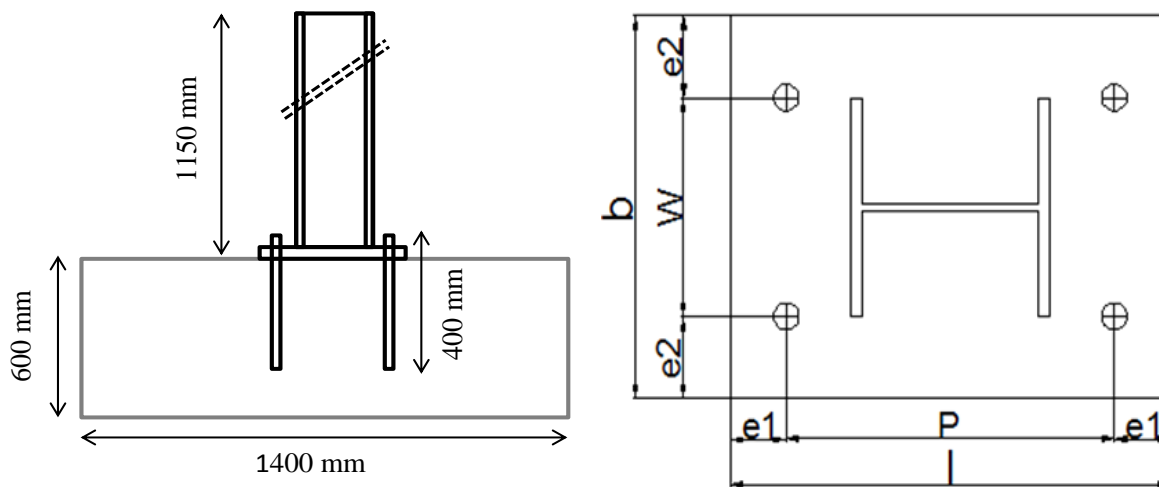


Figure 3. Geometry of the tested specimen

Table 1. Characteristics of the tested specimen

Specimen	Column	Rods	l(mm)	b(mm)	p(mm)	W(mm)	e1(mm)	e2(mm)	tp(mm)
I	HEA160	4	335	280	245	160	45	60	15

### 3.3. Numerical Model

The 3D finite element model was developed under the Ansys code in order to study the behavior of the column base, while taking into account the geometric and material non-linearities; the effect of contact between the various elements was also taken into consideration. In the finite element model, all the connection components were perfectly joined or in good contact, with or without friction. In this case, it should be specified that the column and base plate were in perfect connection, the base plate and washer were in contact, the base plate and concrete were in frictional contact, and finally the anchor rods and concrete were in frictional contact. It should be noted that solid finite elements with 8 nodes and three degrees of freedom per node, were used. In the Ansys code, the finite element is known as Solid 45 [32]. Figure 3 depicts a rectangular optimized mesh that was developed for all parts of the connection. In

addition, surface-to-surface contact was generated for all elements. Moreover, the applied compression axial load F1 was equal to 34 kN according to the experimental test. Finally, the vertical and horizontal loads F1 and F2 were generated in imposed displacements (Figure 4).

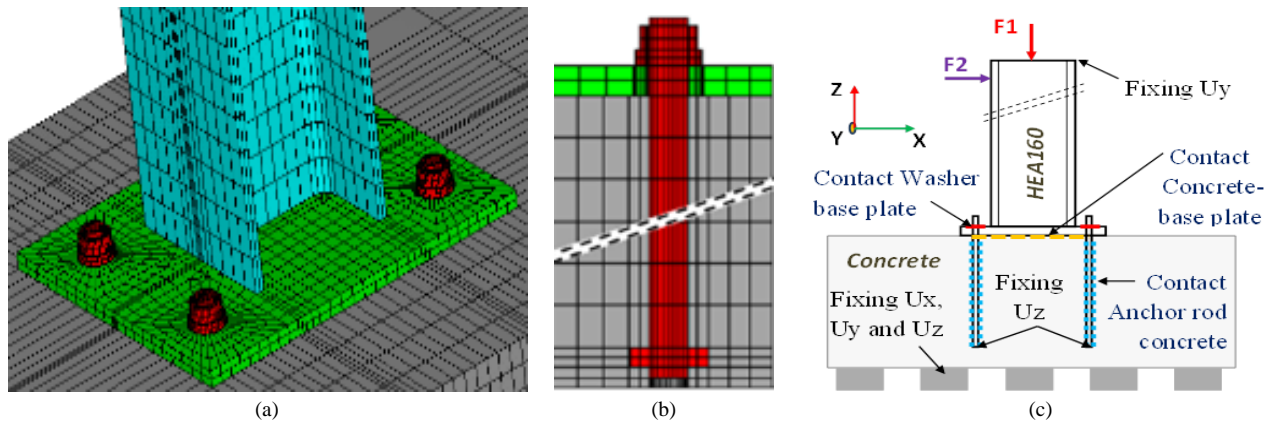


Figure 4. Meshing of the various connection parts and boundary conditions of the model

### 3.4. Material Behavior Laws

The mechanical characteristics of the steel elements used are as follows:  $E = 210000 \text{ MPa}$ ,  $\nu = 0.3$ ,  $f_y = 358 \text{ MPa}$ ,  $f_u = 551 \text{ MPa}$  which were defined by an elasto-plastic constitutive law with hardening. The concrete block was considered as homogeneous, elastic and isotropic, with an elastic modulus equal to  $30000 \text{ MPa}$ . The anchor rod was homogenous with constant unthreaded diameter of  $20 \text{ mm}$  and a length of  $400 \text{ mm}$ . It was made of 8.8 class, with a prestressing equal to 80% of the elastic limit.

### 3.5. Description of the Applied loads to the Numerical Model

The loading was applied in successive stages. First, the prestressing was applied on the anchor rods; then, a compressive force generated in imposed and constant displacement was applied on the head of the column; finally, a horizontal force (imposed displacement) was exerted at the top of the column thus generating a bending moment at the base of the column (Figure 5).

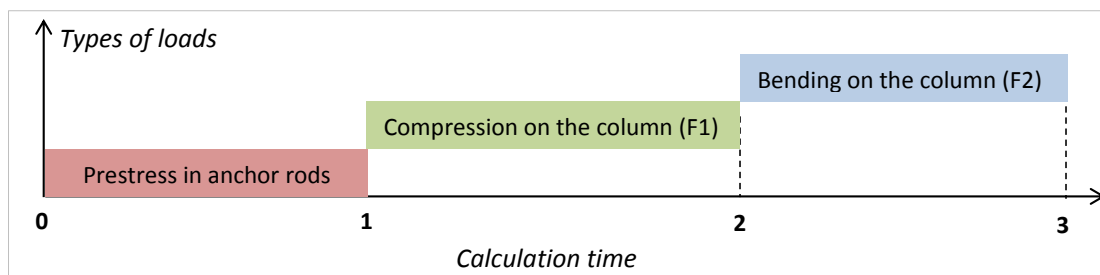


Figure 5. Time loading procedure in the numerical model

### 3.6. Analytical Calculation Method of Moment Resistance and Initial Stiffness

The analytical calculation of the initial stiffness and column base resistance was performed in accordance with the component method proposed by Eurocode 3 (EC3) (EN-1993-1-8) [5]. Once the formations of each component were determined, they were associated in series or in parallel in order to obtain the overall behavior of the column base connection (flexural strength and bending stiffness). The initial stiffness  $S_{j,ini}$  and the moment resistance  $M_{j,Rd}$  can be determined under equilibrium conditions, and expressed as follows:

$$S_{j,ini} = \frac{E \cdot z^2}{\mu \cdot \left( \frac{1}{k_{c,l}} + \frac{1}{k_{c,r}} \right)} \cdot \frac{1}{1 + \alpha_k} \quad (1)$$

$$M_{j,Rd} = \min \left( \frac{F_{t,Rd} \cdot z}{\frac{z_c}{e} + 1}, \frac{-F_{c,Rd} \cdot z}{\frac{z_t}{e} + 1} \right) \quad (2)$$

here  $E$  is the steel elastic modulus,  $\mu$  is the stiffness ratio,  $\alpha_k$  is a quantity that depends on the type of loading, and finally  $k_{c,l}$  and  $k_{c,r}$  are stiffness factors that can be found in Tables 6.11 and 6.12 of EN 1993-1-8 [5].

Furthermore,  $F_{t,Rd}$  is the tensile strength of the T-stub in tension and  $F_{c,Rd}$  is the compressive strength of the T-stub in compression,  $Z$  is the sum of  $Z_t$  and  $Z_c$ , and  $e$  is the eccentricity of the applied load, as shown in Figure 6.

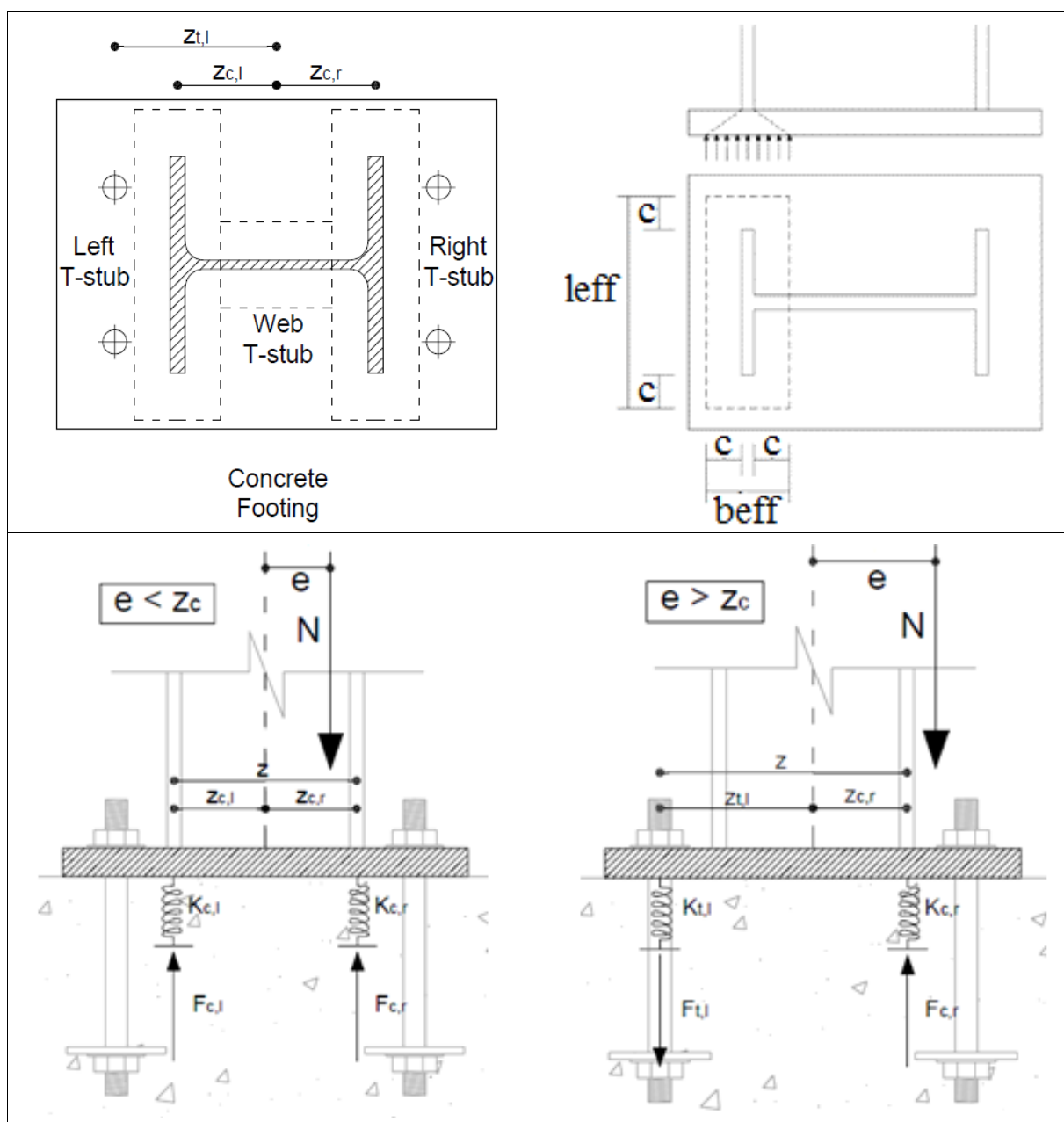


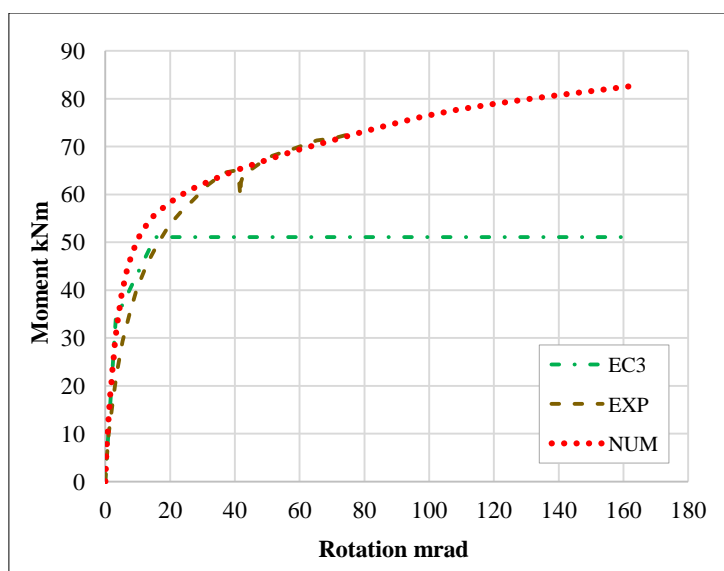
Figure 6. Mechanical model of column bases according to Eurocode 3 [5]

### 3.7. Numerical Analysis Results

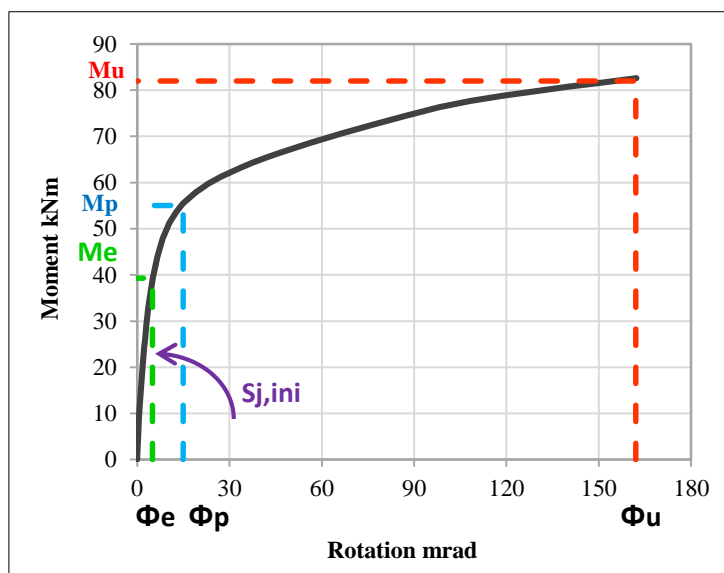
Figure 7-a, shows a comparison between the experimental, numerical and analytical moment-rotation curves of Eurocode 3 (EC3). It is easy to notice that the initial stiffness, according to EC3, is higher by about 12% than that of the numerical model, and by 25% than that obtained from the experimental test. The findings show that the initial stiffness of the numerical curve is between the analytical curve proposed by EC3 and the experimental curve. However, in the plastic part, the numerical curve is close to the experimental curve; a difference of 1.5% is then observed by comparison with the value found experimentally.

Figure 7-b presents the following parameters: the initial stiffness  $S_{j,ini}$  represented by the initial slope of the elastic part of the moment-rotation law. The elastic moment  $M_e$  which represents the limit of the elastic part of the curve, the ultimate moment  $M_u$  which corresponds to the maximum load that the connection can reach, the plastic moment  $M_p$  corresponding to the resistant moment  $M_{j,Rd}$  resulting from the analytical calculation of EC3 and which is obtained from the intersection between the elastic slope (initial stiffness) and the slope representing the plastic phase. The parameters characterizing the moment-rotation curve of the resulting joint obtained numerically and from the experimental tests [9] are shown in Table 2.





(a) Curve M- $\phi$  (EXP, EC3, NUM)



(b) Representation the  $M_e$ ,  $M_p$ ,  $M_u$  in the curve M- $\phi$

Figure 7. Validation of the model and characteristics of curve M- $\phi$

Table 2. Comparison of EC3, experimental and numerical results

	Numerical	EC3	<u>Numerical</u> EC3	Experimental	<u>Numerical</u> Experimental
Initial stiffness $S_{j,ini}$ (kN.m/mrad)	8.8	10	-12%	7.5	+17%
Moment $M_p$ or $M_{j,Rd}$ (kN.m)	55	51	+7%	54.2	+1.5%

Based on the results presented in Figure 7-a and Table 2, it can be seen that there is correlation between the numerical, analytical and experimental results in the elastic and plastic phases. Other differences found in the comparison may be due to a number of factors, such as pre-stressing of rods, contact and friction between the elements and initial imperfections. Overall, it can be said that the proposed finite element model gives an accurate representation of the behaviour of joints under bending moment and compressive load.

#### 4. Mechanical Behavior of the Column Base Plate

The FEM model was adopted to conduct a detailed analysis of the specimen previously described in Figure 4 in order to better understand the behaviour of each component of the column base connection in the elastic domain and the plastic domain, until reaching a damage mechanism. The elements considered in this study are the base plate (elasto-plastic deformation, failure modes, prying effect, stress distribution and effect of thickness) and the anchor rods (internal forces, internal stresses and local time).

### 4.1. Deformation of the Base Plate

The finite element deformation model is presented for the point of maximum loading that corresponds to  $M_u$ ; this maximum loading caused the deformation of the base plate and anchoring rod, along with a yielding of this rod (Figure 8-a). The point of maximum displacement  $U_z$  of the order of 25 mm is located at the base of the column. Moreover, the base plate deformation generated the plastic deformation of the taut rod R1 that is subjected to a local bending moment and also to the tensile force. In addition, the flexibility of the plate that is in contact with concrete greatly contributes to stiffness and resistance and helps to increase the intensity of the applied compressive force [33]. As for Figure 8-b, it shows the deformation of the base plate in the plane of the column web for the different loading phases ( $M_e$ ,  $M_p$ , and  $M_u$ ).

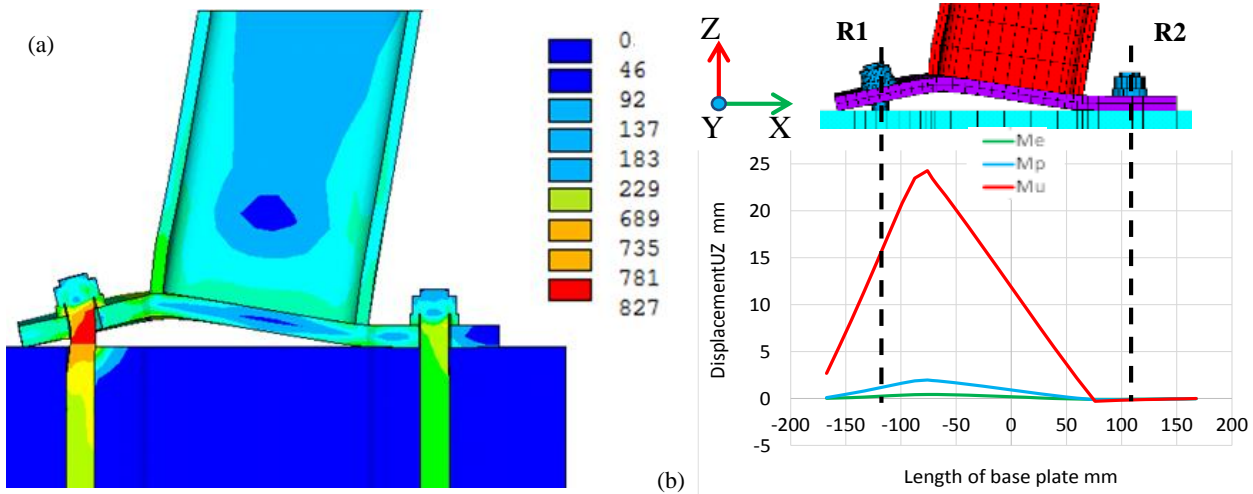


Figure 8. Model deformation and von Mises stress distribution

### 4.2. Failure Modes of the Base Plate

Considering the previously described base plate, and using the Eurocode 3 [5] analytical formulation to determine its failure mechanism, it becomes possible to deduce the set of possible failure modes as follows:

$$\text{Mode 1: } F_{1T,Rd} = \frac{(8n-2ew) * (M_{pl1,Rd})}{(2mn) - ew * (m+n)} = 363 \text{ kN} \tag{3}$$

$$\text{Mode 2: } F_{2T,Rd} = \frac{2 M_{pl2,Rd} + n \sum F_{t,Rd}}{m+n} = 315 \text{ kN} \tag{4}$$

$$\text{Mode 3: } F_{3T,Rd} = \sum F_{t,Rd} = 452 \text{ kN} \tag{5}$$

It can therefore be said that failure mode 2 (formation of a partial mechanism that is accompanied by failure of the rods under tension thus preventing the development of the full yielding mechanism) is critical, which gives the tensile design strength  $F_{T,Rd} = 315.2 \text{ kN}$  on the tension side of the column base connection. On the other hand, using the finite element model, the tensile force of the T-section obtained numerically for the last loading step, gives  $F_t$ , numerical =  $F_{bz} - F_{tz} = 331 \text{ kN}$ , where  $F_{bz}$  is the axial force in the rod and  $F_{tz}$  is the lever effort in the tension zone. These two quantities are determined numerically. It should be noted that the failure mode obtained numerically corresponds to mode 2 (partial mechanism) of the analytical calculation according to EC3. This is confirmed in Figure 9 with shows the yielding of the base plate in bending as well as the yielding of the anchor rod. It can therefore be concluded that the numerical failure mode is similar to that of EC3.

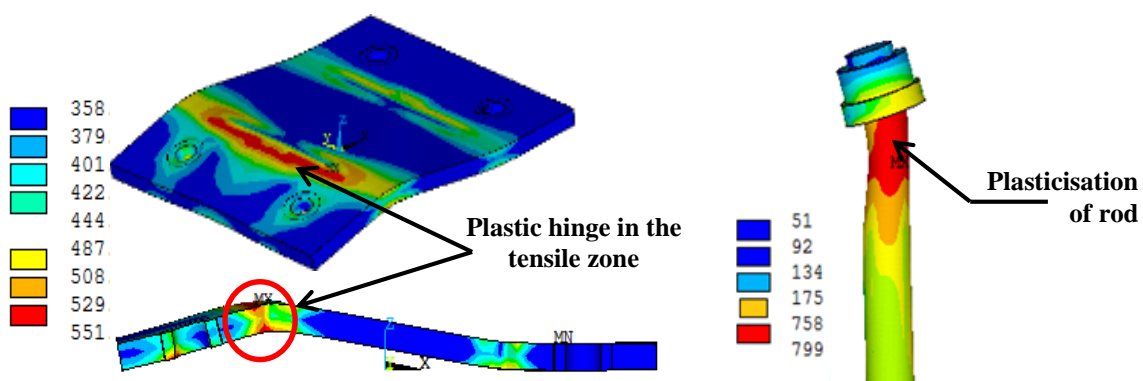


Figure 9. Numerical representation of the failure mode with von Mises stress distribution



Figure 10 displays the moment-rotation law that describes the behavior of the column base plate connection as well as the evolution of the failure modes. Points p1, p2, p3 and p4 represent the various unfolding phases of the failure modes in the column base connection. These findings were then compared with the experimental and analytical (EC3) ones. From the numerical point of view, point p1 represents the beginning yielding of the base plate at the connection with the column in the tension zone. Point p2 represents the beginning of yielding of the rod in the tension zone. Point p3 corresponds to the significant anchor rod yielding in the tension zone of the connection, and finally point p4 represents the plastic mechanism of the base plate at the connection with the column in the tension zone.

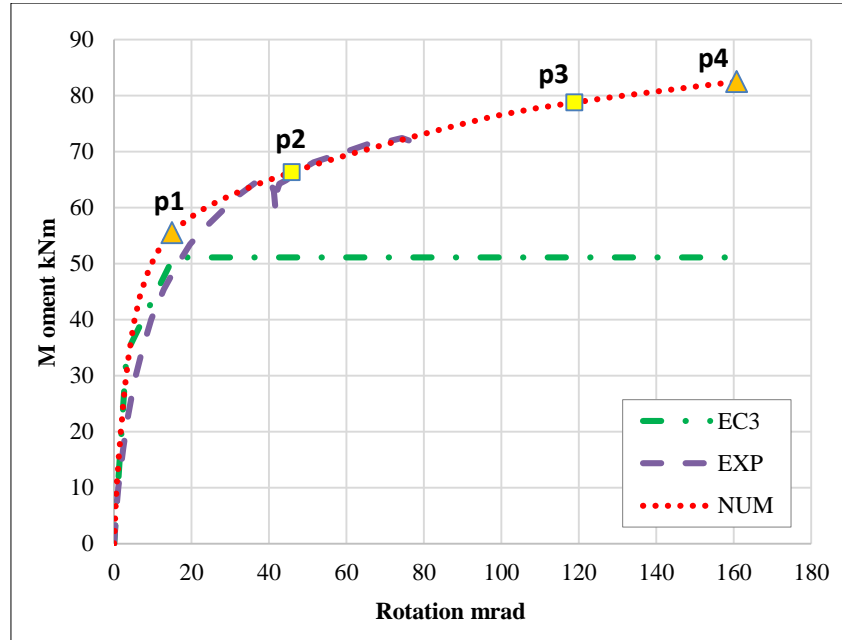


Figure 10. Comparison of numerical, experimental and EC3 moment-rotation curves

### 4.3. Prying Action Effect

In this part, the pressure distribution at the contact of the base plate with concrete due to the prying force in the column base connection is analyzed. It should be noted that the pressure due to the prying forces develops in the tension zone between the pre-tensioned anchor rods to the end of the base plate. In the compression zone, the center of compression is at the column flange, as shown in Figure 11.

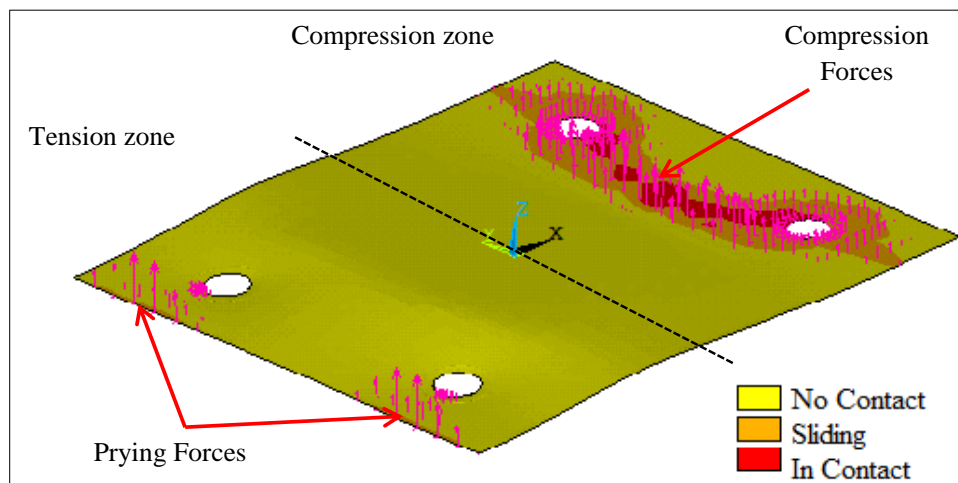
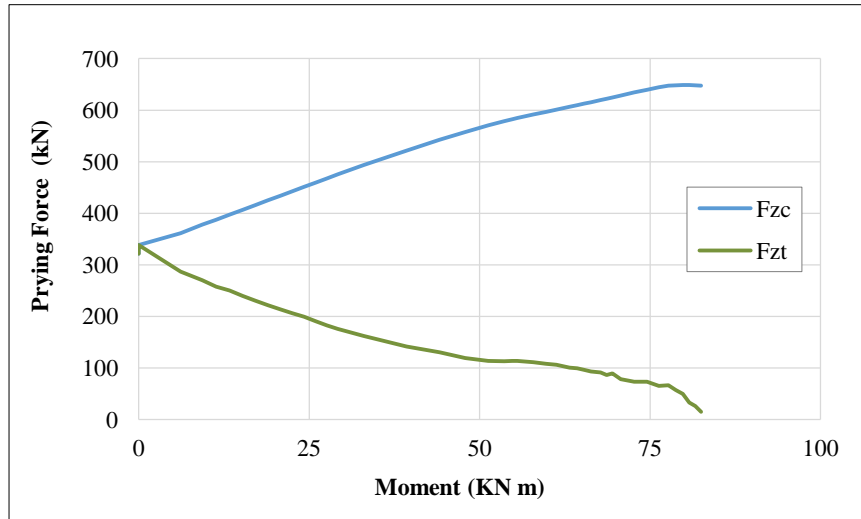


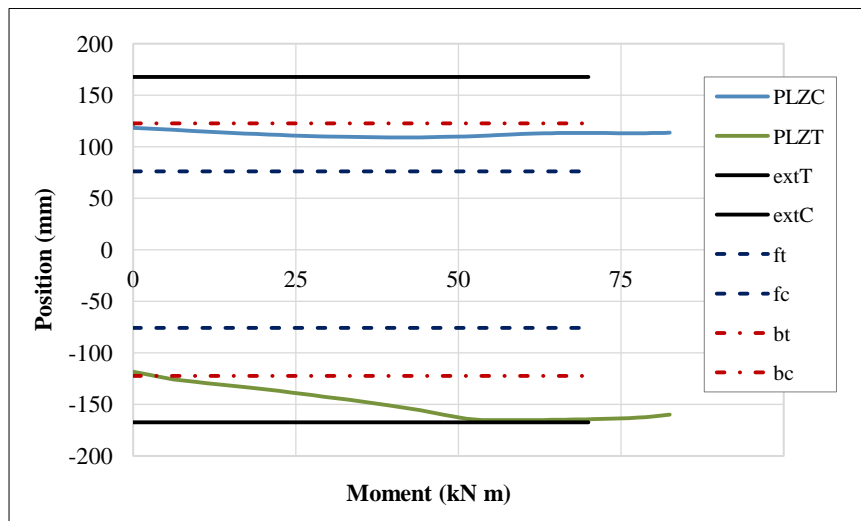
Figure 11. Contact pressures of the base plate with concrete (view on the lower fiber)

If prying is present in a column base, it gives either failure mode 1 or failure mode 2 (Eurocode 3). One should note that failure mode 2 is associated with increased tensile forces in the anchor rods due to deformation of the base plate in bending, which causes separation with concrete, except at the edges of the plate where the prying effect appears. This effect causes an increase in the tensile force of the same value in each anchor rod. It should be emphasized that when the plate deformations are significant, there may be some significant bending of the anchor rods.

As the studied connection has prestressed rods, the initial value of the prying force  $F_{zt}$  and compression forces  $F_{zc}$  is equal to the initial prestressing forces multiplied by the total number of anchor rods (Figure 12-a). The presence of the prying force in the tension zone has been observed since the start of loading. Its value decreases as the load increases because the bending deformation of the base plate becomes greater (separation between the plate and the concrete in the contact zone). However, in the compressed zone, the prying force  $F_{zc}$  increases because the plate remains in contact with concrete throughout the entire loading process. The prying effect, which is due to the existing prestressing, begins at the axes of the anchor rods and then starts moving to the outer edge of the base plate in the tension zone PLzt, as shown in Figure 12-b. However, in the compressed zone, the position of PLzc evolves near the axis of the rod, which is different from that of Eurocode 3 (EC3) [5] which locates it on the axis of the compressed flange of the column.



(a) Variation of the prying effort versus the applied moment



(b) Variation of the prying position versus the applied moment

**Figure 12. Prying effect in the column base plate connection**

Note that:

- $F_{zc}$  is the prying effort in the compressed zone
- $F_{zt}$  is the prying effort in the tension zone
- $PL_{zc}$  is the prying position in the compressed zone
- $PL_{zt}$  is the prying position in the tension zone
- $extT$  represents the end of the plate in the tension zone
- $extC$  stands for the end of the plate in the compressed zone
- $ft$  is the position of the column flange in the tension zone
- $fc$  is the position of the column flange in the compressed zone
- $bt$  is the position of the anchor rods in the tension zone
- $bc$  is the position of the anchor rods in the compressed zone.

Figure 13, depicts the evolution of the plate-concrete contact surface according to the different loading steps. It is noted that, before the horizontal loading is applied, the plate is subjected to the column compression only. Next, the prestressing of the anchor rods generates some localized pressures around the holes of the base plate. During the evolution of the horizontal loading, and hence of the bending moment on the connection, the base plate deformation develops by zones until it reaches plastic deformations, which generates a concentration of pressures on the column flange (compressed zone) and on the base plate edges (prying effects on the tensile part).

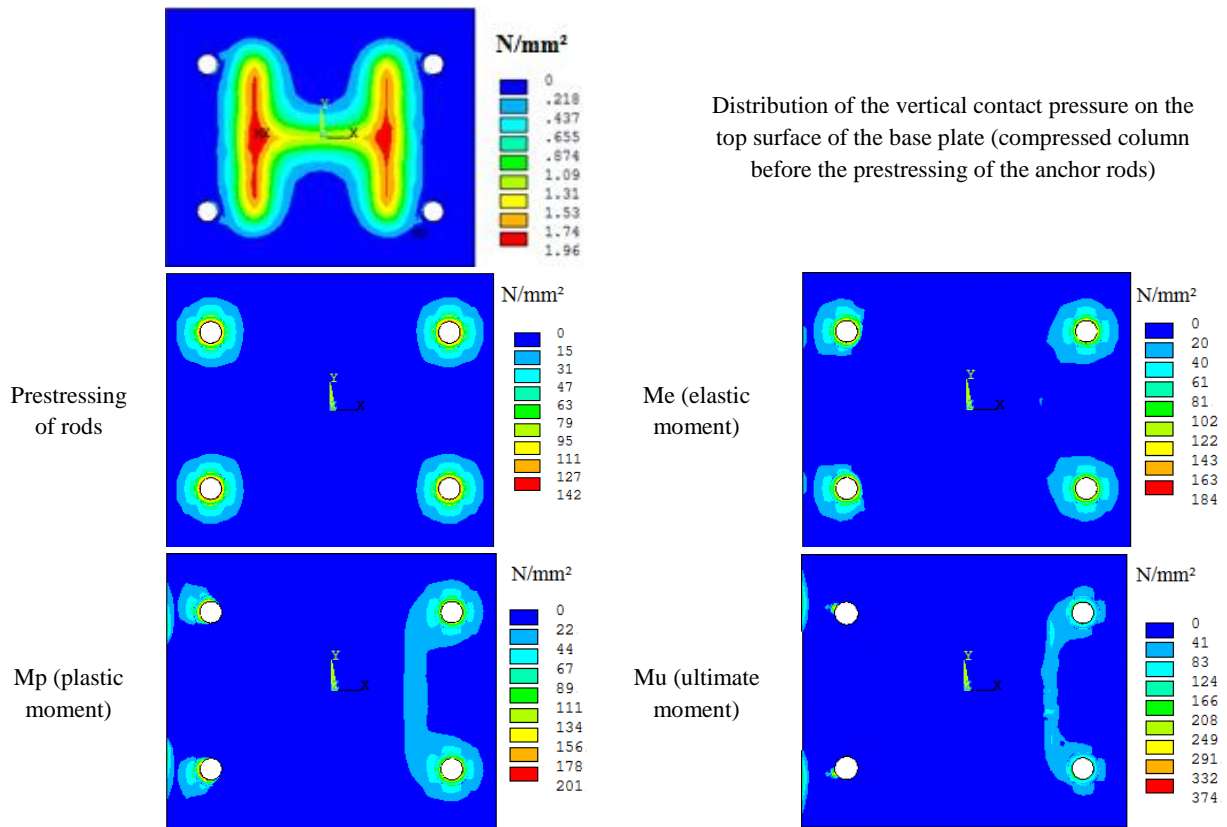


Figure 13. Evolution of the contact pressure on the column base plate, for different moment values

#### 4.4. Forces in the Anchor Rods

It is important to understand the behavior of the anchor rod in the tensile zone. Figure 14 shows the evolution of the forces present in the strained rod, on the one hand, and those in the compressed rod, on the other, as a function of the moment applied to the column base plate. In addition, the force in the rods starts with a value of about 160 kN which corresponds to the prestressing applied in the rods. Note also that for the two rods, the variation of the force is not noticed until a certain level of loading is reached. Beyond that force, the strained rod ( $F_{zt}$ ) shows a variation in the continuous force that is quasi-proportional to the applied moment, but with a rather exponential trend, up to the value of 201kN. This would cause the force to decrease as a result of rod deformation in the tensile zone. However, for the rod located in the compressed zone ( $F_{zc}$ ), the force starts with the prestressing value. Then, a weak unloading of the rod takes place as a result of the bending deformation of the base plate. Note that  $F_t$  is the ultimate force in the anchor rod;  $F_t = 0,9.fub.A$ .

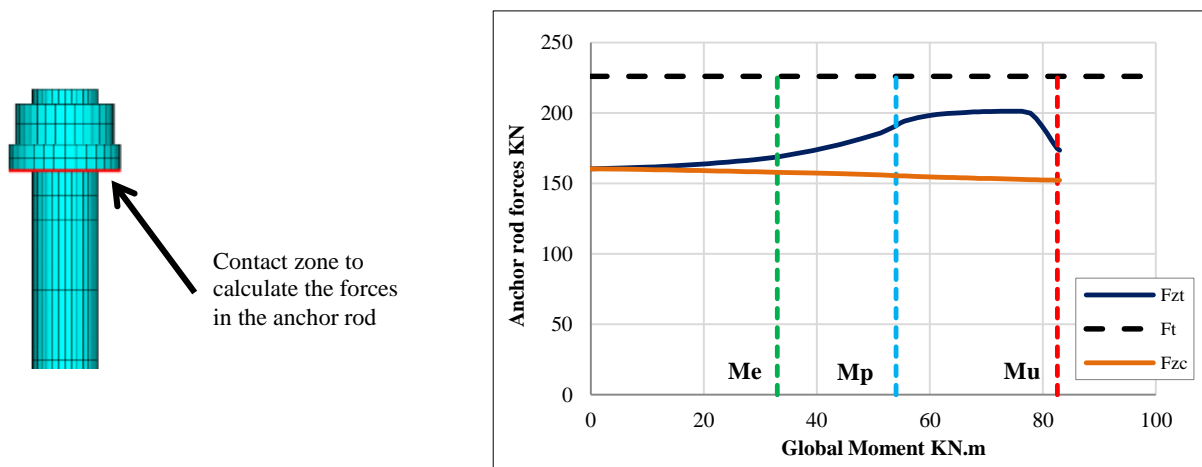
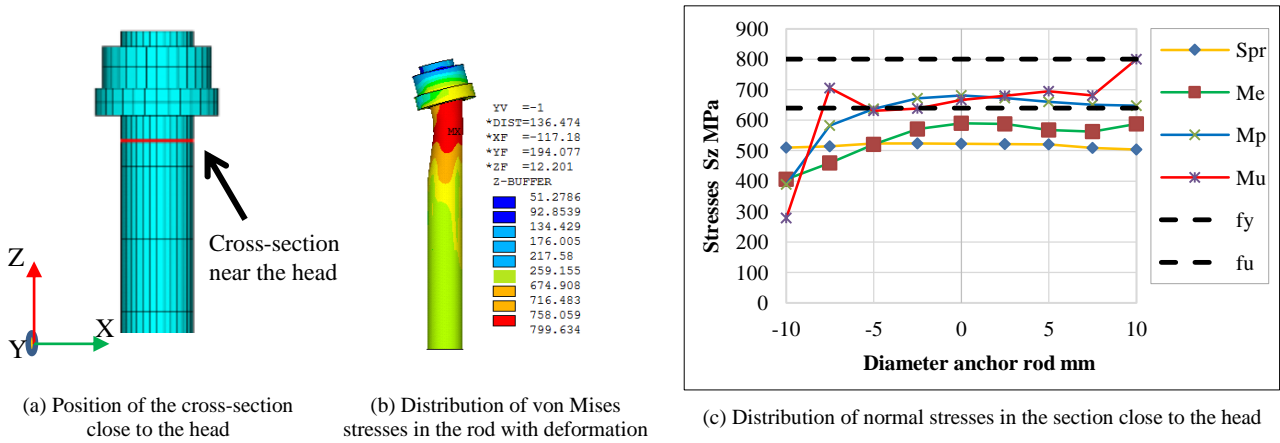


Figure 14. Evolution of the axial force in the rod as a function of the moment applied

**4.5. Stress Distribution in the Anchor Rod**

The idea developed in this study consists in analyzing the stress distribution in the axial direction of the rod (Z axis), by choosing two observation sections, to determine the effect of the cutting section close to the head and far from the column head, and also to see if the same stress status is found for a section close to the head and for a section far from the head (Figures 15 and 16). It was found that, for the section close to the head, the stresses due to the elastic (Me), plastic (Mp) and ultimate (Mu) moments of the connection are not distributed in a homogeneous way, which confirms the presence of a local bending moment in the rod, in addition to tension. This moment therefore favors the failure of the anchor rod. It is useful to remember that the EC3 does not take into account the local moment in the rod.



**Figure 15. Distribution of stresses in the rod (cross-section close to the head)**

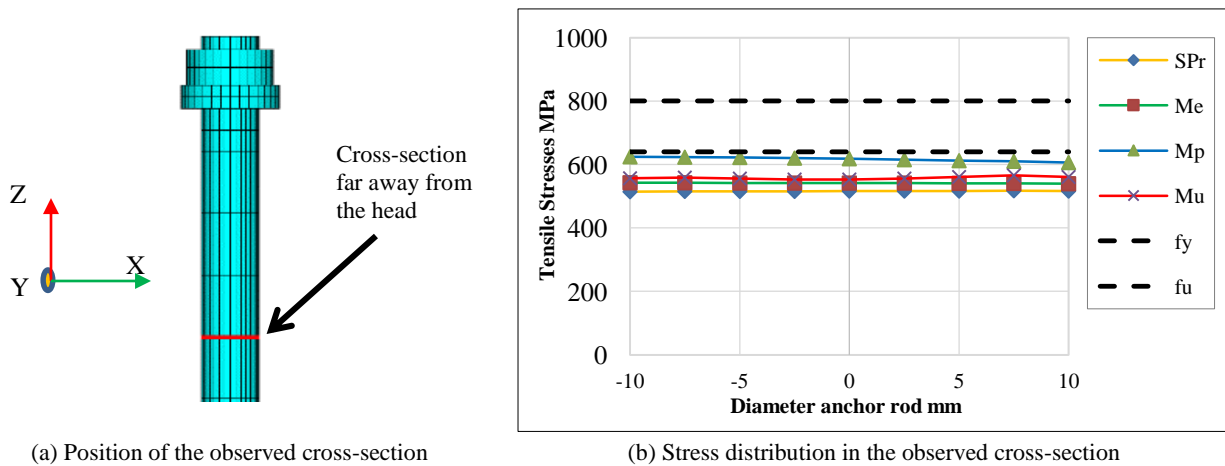


**Figure 16. Distribution of stresses in the rod (cross-section far away from the head)**

Figure 16 shows the stress distribution in a cross-section far away from the rod head (nut in our case). It can be seen that the tensile stresses show uniform distribution on the cross-section.

Note that:

- Me: represents the stresses due to the elastic moment
- Mp: represents the stresses due to the plastic moment
- Mu: represents the stresses due to the ultimate moment
- Spr: represents the stresses due to the prestress in the rod

**4.6. Bending Moment of the Anchor Rod without Prestressing**

The same specimen was studied using similar anchor rods without prestressing (M20 grade 8.8). The effect of the moment on the anchor rod and the internal stress distribution were analysed.

It is worth emphasizing that the influence of the moment on the tension rod is quite significant (Figure 17 and Table 3). For the specimen analyzed, the stresses due to the bending moment and normal force represent respectively 2/3 and 1/3 of the total axial stress Szz. Remember that Eurocode 3 only takes into account the normal force and neglects the presence of bending on the anchor rod. Moreover, the yielding or failure of the rod can be caused by the presence of a large local moment.

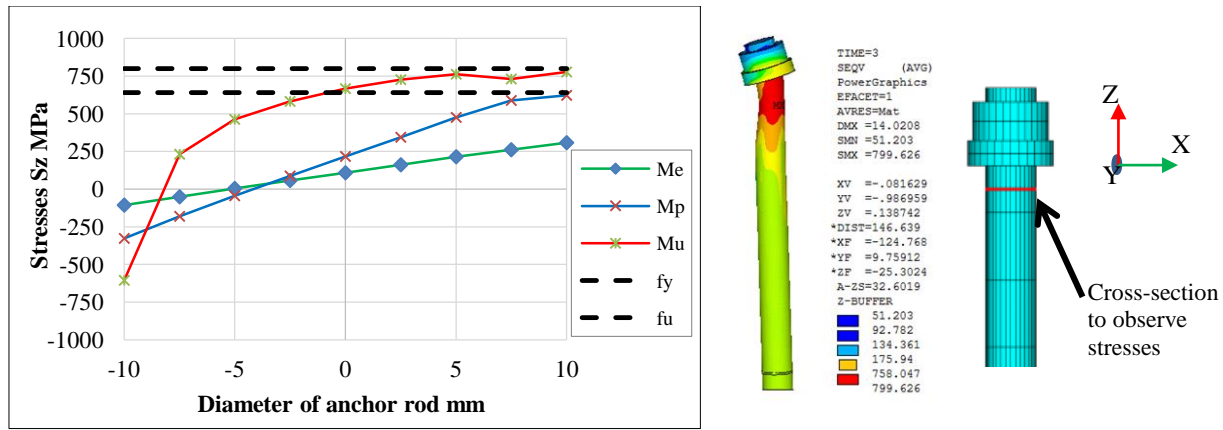


Figure 17. Stress distribution the rod in the tensile zone

Table 3. Axial stress with values due to normal force and bending moment

Stresses in extreme fibers		Stress $S_N$ (MPa)	Stress $S_M$ (MPa)
Stress $S_{Top}$ (MPa)	Stress $S_{Bott}$ (MPa)	$(S_{top}+S_{bott})/2 = 79.1$	$(S_{top}-S_{bott})/2 = 160.4$
+239.5	-81.3		

4.7. Behaviour of Anchor Rods

Figure 18 shows the elongation of the stretched rod in the vertical direction (Z), with the three parts of the anchor rod, namely tp: part in the plate, anch: anchored, part, and full = tp+anch. This figure indicates that the force in the rod is greater than the prestress force; it can reach the value of 200kN, which makes it possible to have a maximum elongation of 5mm over the entire length of the rod. It should also be noted that the internal force decreases at the end of the course due to the yielding of the rod, and in this case the elongation increases and can reach the value of 9mm. The deflection at the deformed plate is quite large; it is almost equal to the elongation at the rod anchor.

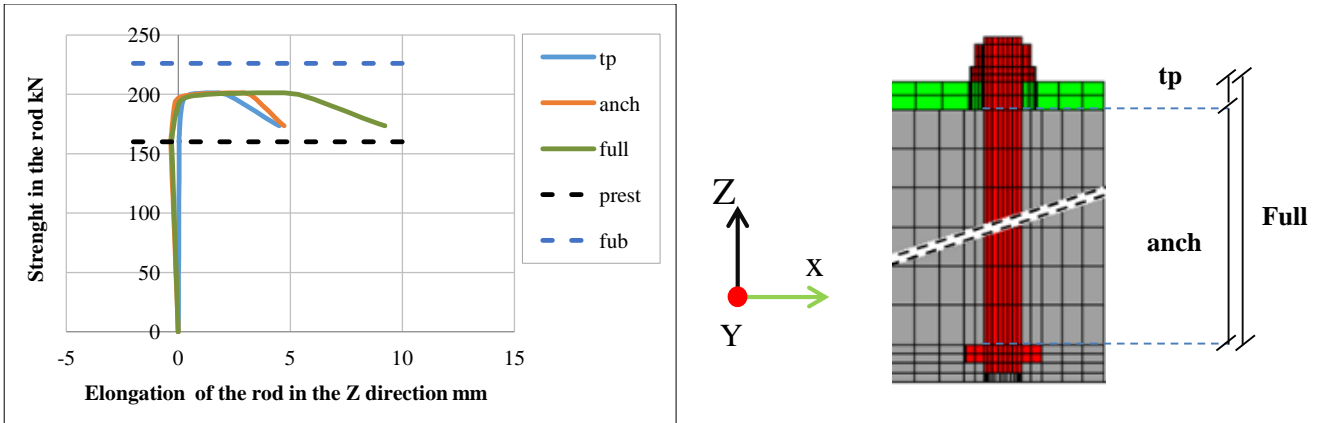


Figure 18. Force-displacement curve of the anchor rod

5. Study of the Effect of Stiffening on the Behaviour of the Column Base Plate

It has been shown that the base plate is the main component influencing the stiffness and strength of the column base connection. For this, it was deemed interesting to study the eventuality of reinforcing this plate with stiffeners welded to the base plate and column.

It is worth recalling that, the purpose of this study is to investigate the effect of the stiffeners on the mechanical behavior of the column base connection. Thus, the influence of the stiffener height and its shape on the connection and on the prying effect is analysed.

The basic geometric characteristics of the connection are not changed. A bending moment and a compressive force of 34kN were applied to investigate the behavior of the stiffeners in the column base. In this case a 15mm S235 grade base plate and M20 8.8 grade rods, with a triangular stiffener of 8mm thickness, 90mm width and 100mm height, were used.

### 5.1. Effect of Stiffener Position on Connection Behaviour

Figure 19 shows the studied specimens of column bases, with different positions of stiffeners (SR: without stiffener, R-TC: with two stiffeners, R-C: stiffener in the compressed zone, and R-T: stiffener in the tension zone).

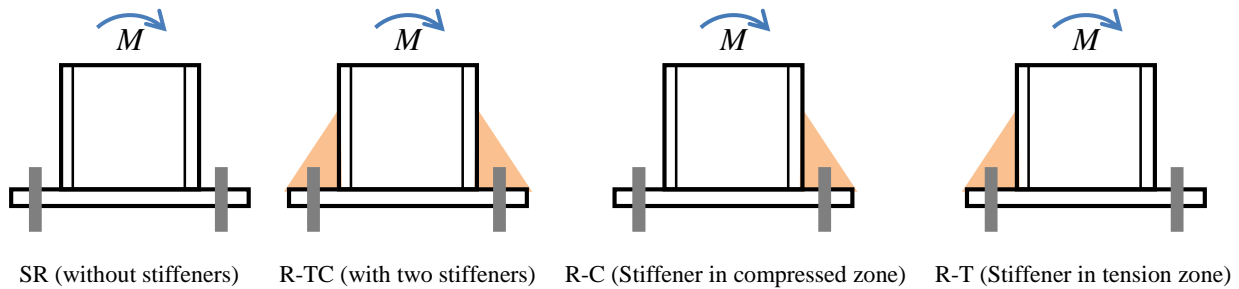


Figure 19. Positions of column base plate stiffeners

Figure 20 presents the moment-rotation curves of the stiffened and unstiffened connections with different stiffener arrangements. The results obtained show that the specimens with stiffeners exhibit higher values of initial stiffness and bending resistance. It is also noticed that the specimen with stiffener in the tension zone plays a fundamental role in the resistance of the connection. Besides, the stiffener in the compressed zone gives resistance lower than the previous one but higher than the specimen without stiffeners. As expected, the connection with stiffeners on both sides of the column is the most efficient and most resistant.

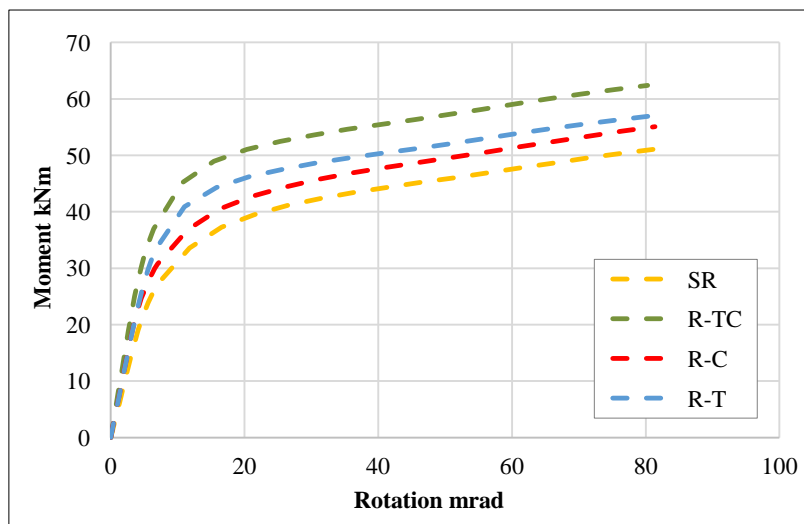


Figure 20. Effect of stiffener arrangement on the moment-rotation behavior

Table 4 presents the results of the effect of the stiffeners on the column base connection considering the initial stiffness and plastic moment. The compared values use the unstiffened connection (SR) as reference. It can be observed that the specimen (R-TC) performs best in terms of initial stiffness (+43%) and bending resistance (+32%). In addition, the model with stiffener in the tension zone (R-T) is relatively more efficient than that in the compressed zone (R-C).

Table 4. Effect of stiffener on initial stiffness and plastic moment

Specimen	Plastic moment $M_p$ , kN.m	Difference/SR %	Initial stiffness $S_{j,ini}$ kN.m/mrad	Difference/SR %
SR (without stiffeners)	28	-	4.70	-
R-TC (with two stiffeners)	37	+32	6.72	+43
R-C (stiffener in compressed zone)	31	+10.71	5.62	+19.58
R-T (stiffener in tension zone)	34	+21.43	5.77	+22.77

### 5.2. Effect of Stiffener Position on Prying Action

Prying plays a fundamental role in the strength of the column base plate connection. It depends on several parameters. The influence of the stiffener position on the prying effect is analyzed considering 4 types of stiffening



(SR, R-TC, R-C, R-T). Figures 21 and 22 illustrate the results obtained for the prying force in the tensile and compressed zones and its position. It can be observed that the prying force in the unstiffened specimen (SR) is the greatest due to the deformation of the unstiffened plate deformation. It is followed by the RC specimen (stiffener in compressed zone), the R-T (stiffener in the tensile zone) and the R-TC specimen (stiffeners in tensile and compressed zones). Thus, the specimen R-TC is the most effective in terms of reducing the prying force (Figure 21).

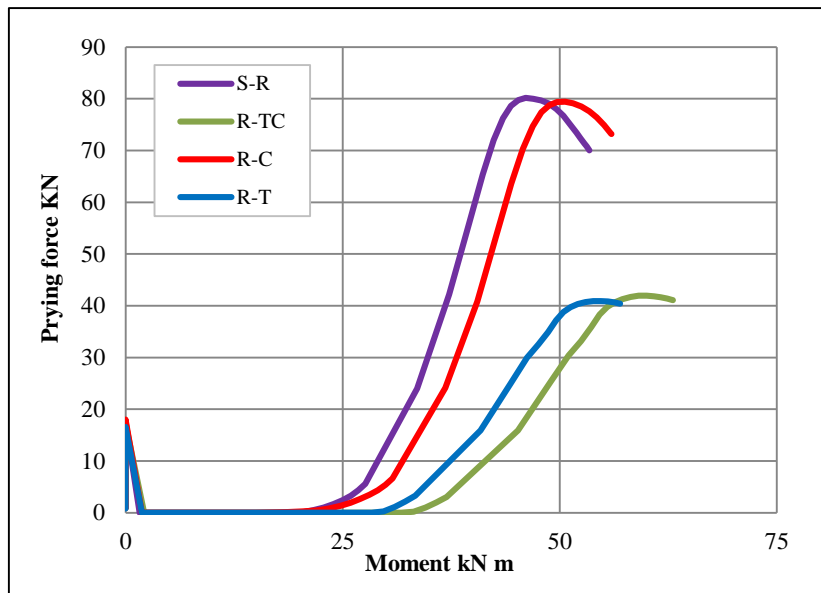


Figure 21. Comparison of prying forces for different types of stiffening

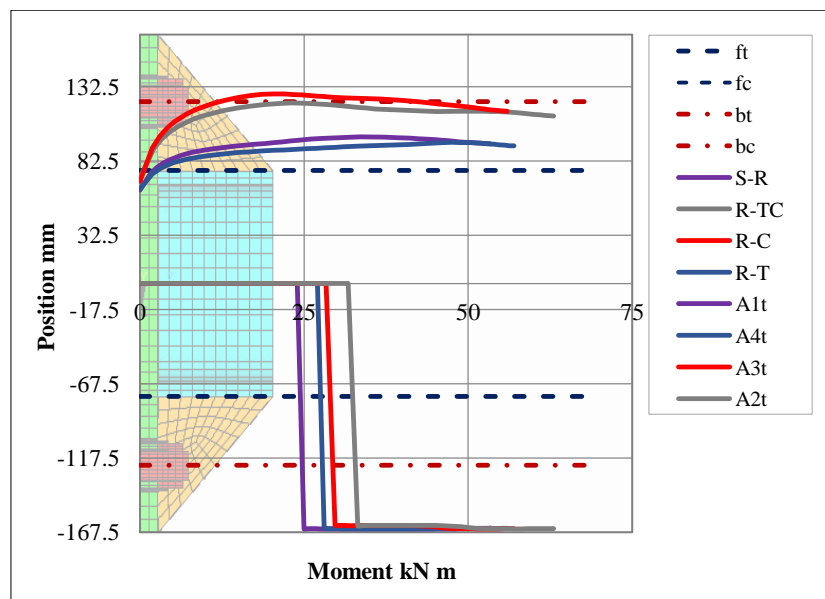


Figure 22. Comparison of prying position and compression center for different types of stiffening

Figure 23 shows the stress distribution in the base plate. With the presence of stiffener, this distribution changes depending on whether it is in the tensile or the compressed zone. Thus, the stiffener in the tensile zone considerably decreases the prying force (Figure 21). However, the stiffener in the compressed zone has no effect on the prying force in the tensile zone. Furthermore, the presence of the stiffener changes the position of the center of compression in the compressed zone (Figure 22). Thus, the center of compression gets closer to the rod for specimens R-TC (with stiffeners in tensile and compressed zones) and R-C (with stiffener in compressed zone). On the other hand, for the specimens SR (without stiffeners) and R-T (stiffener in tensile zone), the center of compression is close to the column flange. The results obtained show that the stiffener reduces the prying force in the tensile zone and also changes the position of the compression center, which provides quite high values of initial stiffness and bending resistance of the connection.

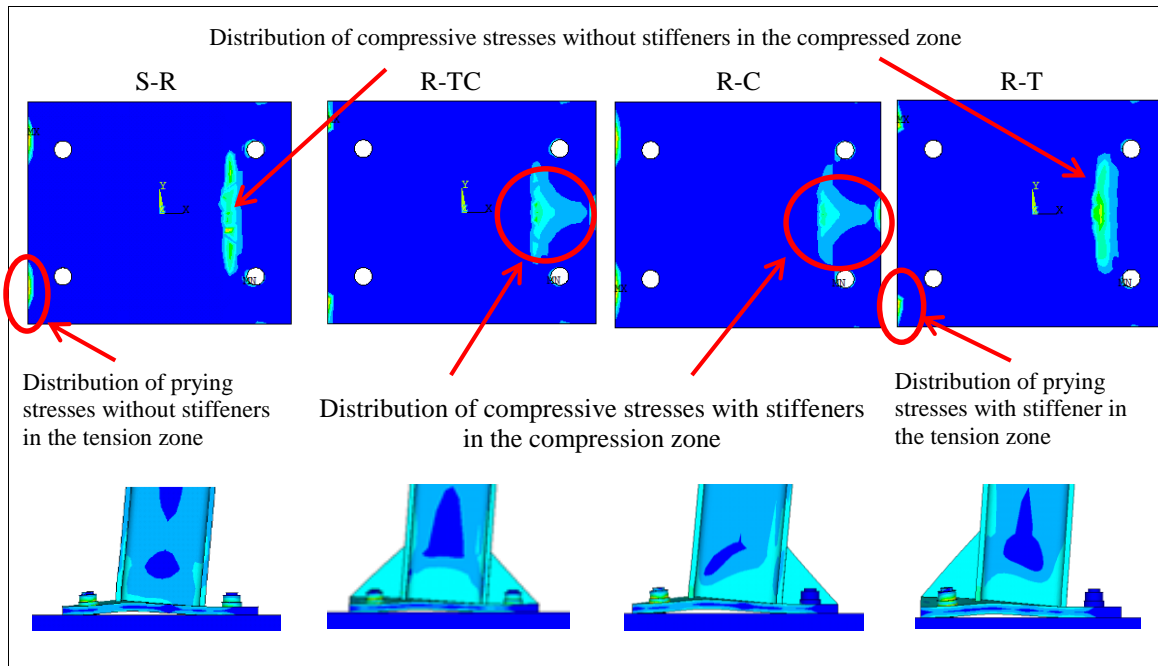


Figure 23. Distribution of prying stresses in the tension zone, and compressive stresses in the compression zone, for different types of stiffening

**5.3. Effect of Stiffener Position on Forces in Anchor Rods**

Figure 24 shows the forces in the anchor rods in tension zone of the connection. The stiffener plays an important role in the resistance of the anchor rods, as clearly shown in Figure 20. It should be noted that the specimen R-TC (stiffeners in the compression and tension zones) gives the highest values of stiffness and bending strength. Also, the rod in the tension zone is less stressed than in the case without stiffeners (SR). This shows that the stiffener plays a significant role in reducing the internal forces in the anchor rod (Figure 24).

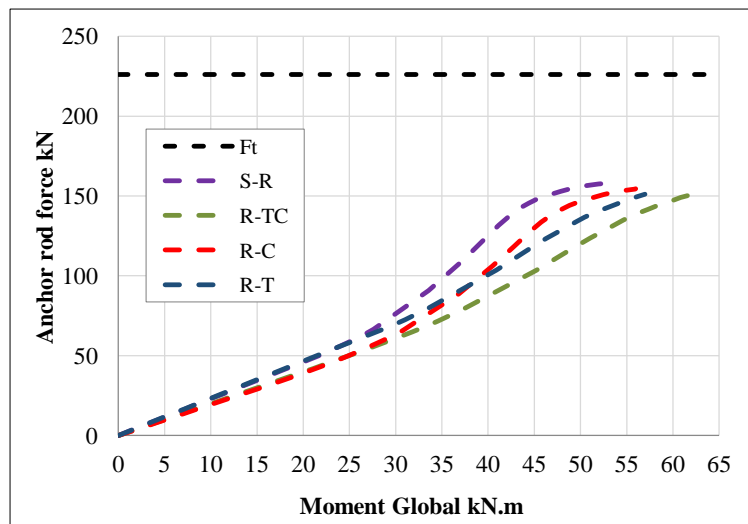


Figure 24. Comparison of the tensile forces in the anchor rods in tension zone for different types of stiffening (Ft: ultimate tensile force in the anchor rod)

**5.4. Effect of Stiffener Height on the Moment-Rotation Curves**

The stiffener height plays a very essential role in the column base connection; it indeed allows minimizing the stress concentration on the column [34]. Afterwards, a triangular stiffener of width  $l_s$ , height  $h_s$ , and thickness  $t_s$  is studied while taking into account the geometric and material characteristics of the column base that has previously been defined (S235), with the plate thickness = 15 mm, M20 grade rod without prestressing. Then, a bending moment and a compression axial force equal to 34kN are applied. The stiffener height  $h_s$  were varied in order to analyze its influence on the behaviour of the connection (Figure 25). The deformation of the column base connection for different stiffener height values is shown in Figure 26.

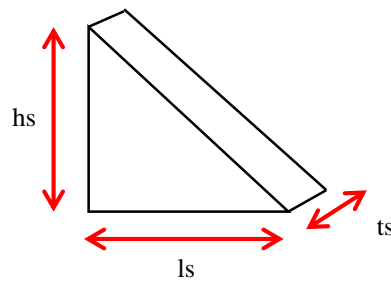


Figure 25. Stiffener geometry

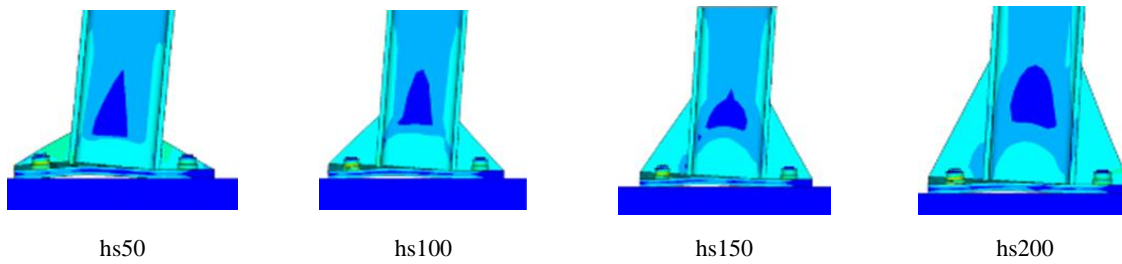


Figure 26. Deformation of the column base connection for different values of stiffener height

Table 5 shows the studied specimens (unstiffened and with two stiffeners) where the stiffeners heights  $h_s$  were varied, while keeping constant the other geometric parameters.

Table 5. Stiffener specimens

Specimen	$t_s$ (mm)	$h_s$ (mm)	$l_s$ (mm)	Base plate thickness (mm)	Rod diameter (mm)
hs50	8	50	100	15	M20
hs100	8	100	100	15	M20
hs150	8	150	100	15	M20
hs200	8	200	100	15	M20
Without stiffener	-	-	-	15	M20

Figure 27 displays the moment-rotation curve of the specimens with different stiffeners heights. By increasing the stiffener height, it can be observed the increase of the initial stiffness and bending resistance of the column base connection. It is also noticed that the curves do not stop with the same moment. This is due to the appearance of a plastic hinge (plasticisation of the base plate) in the connection.

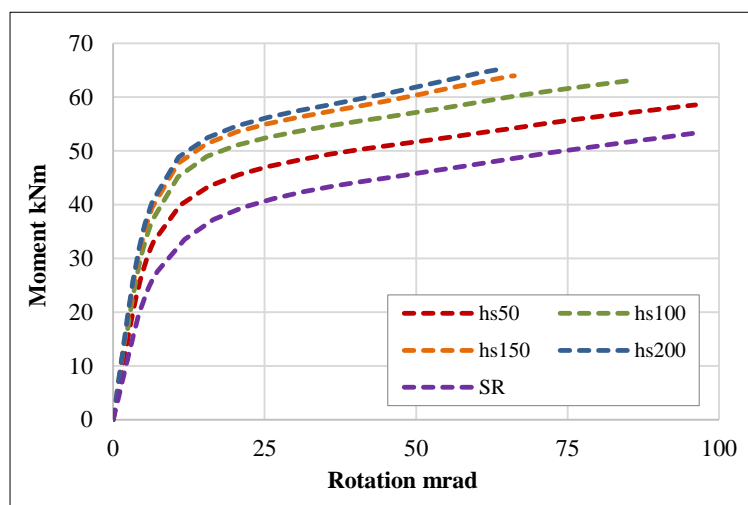


Figure 27. Moment-rotation curve for specimens with different heights of stiffeners

Table 6 summarizes the results of the initial stiffness and plastic moment for the specimen with different heights of stiffeners. The hs200 specimen shows a significant increase in the initial stiffness (+64%) compared to that of the specimen without stiffener; it also exhibits an increase in the plastic moment (+47%). These results confirm the fact

that the stiffener height has a significant impact on the initial stiffness and bending resistance. Obviously, the greater the stiffener height, the smaller its plastic deformation, which allows the stiffener to modify the failure modes in the column base plate.

**Table 6. Effect of stiffener height (hs) on initial stiffness and plastic moment**

Specimen	ts (mm)	hs (mm)	ls (mm)	Initial stiffness $S_{j,ini}$ (kN.m/mrad)	Difference/WS %	Plastic moment $M_p$ (kN.m)	Difference/WS %
Without stiffener	-	-	-	4.70	-	27.59	-
hs50	8	50	90	5.98	+27	33.10	+19
hs100	8	100	90	6.99	+49	36.97	+25
hs150	8	150	90	7.35	+57	39.37	+43
hs200	8	200	90	7.71	+64	40.58	+47

**5.5. Effect of Stiffener Height on Prying Action**

Figures 28 and 29 present the results related to the prying force and its position in the tension zone and compression zone of the column base connection considering different heights of stiffeners. Figure 28 shows the prying force in the tension zone for the specimens with different heights of stiffeners. It can be easily seen that as the height of the stiffener increases, the prying force in the connection decreases. Figure 29 shows the comparison of the prying position and the compression center for different specimens (hs50, hs100, hs150, hs200, SR).

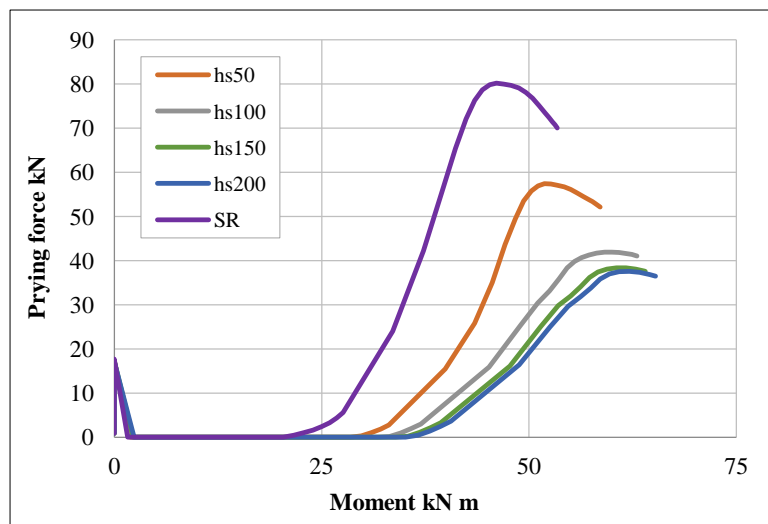


**Figure 28. Comparison of prying force for, different stiffeners heights**

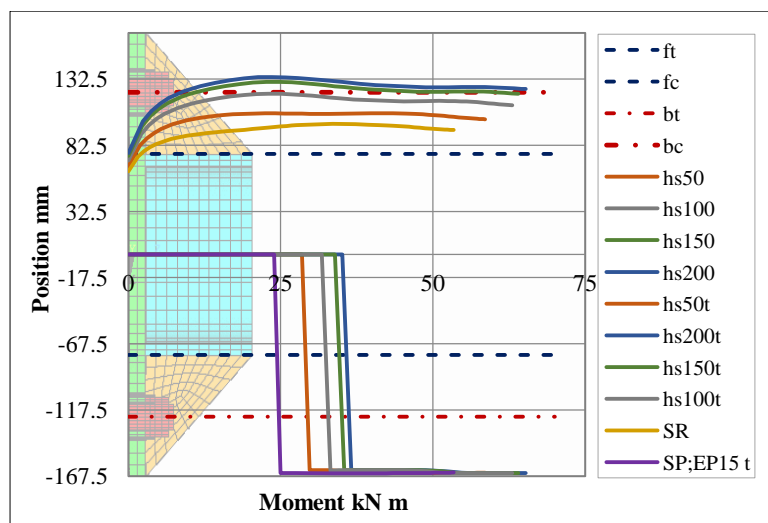


**Figure 29. Comparison of prying position and center of compression for different stiffeners heights**

It is also noted that the position of the center of compression changes as the height of the stiffener increases, while the prying position moves towards the end of the baseplate. Therefore, it may be stated that the stiffener height plays a very important role in the connection. Indeed, it is observed that when the position of the center of compression changes, the prying force in the column base plate connection decreases.

**5.6. Effect of Stiffener Shape on the Moment-Rotation Curves**

Two shapes of stiffeners, rectangular and triangular, with different heights were considered. Table 7 shows the results of the maximum von Mises stresses for these two types of stiffeners.

**Table 7. Effect of stiffener shape on its maximum von Mises stresses**

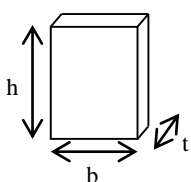
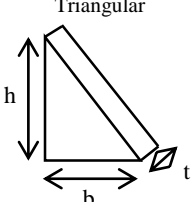
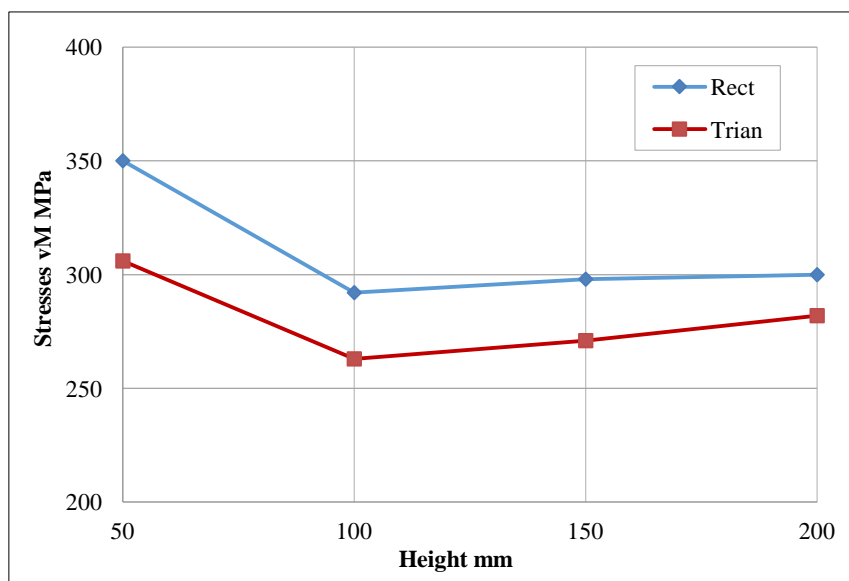
Shape of stiffener	b (mm)	h (mm)	t (mm)	Compressed stiffener max von Mises stress (MPa)	Tensile stiffener max von Mises stress (MPa)
	90	50	8	349	311
	90	100	8	293	243
	90	150	8	298	238
	90	200	8	300	234
	90	50	8	306	298
	90	100	8	262	257
	90	150	8	272	240
	90	200	8	281	262

Figure 30 shows the variation of the maximum von Mises stress as a function of the height of the compressed stiffener. The curve obtained shows that the concentration of the maximum von Mises stresses is higher in the rectangular stiffener. In addition, the maximum von Mises stress is greater for a small height (h = 50 mm), whether for the triangular or rectangular stiffener.



**Figure 30. Maximum von Mises stress in the compressed stiffener**

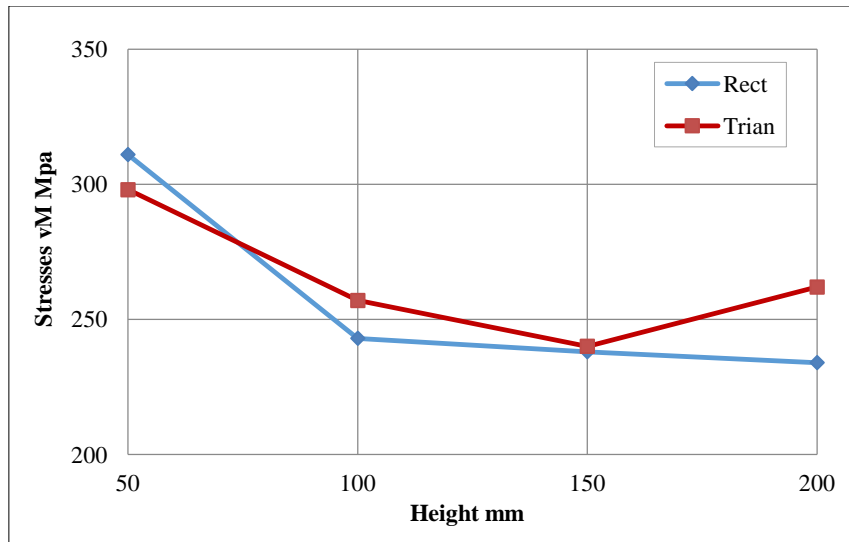


Figure 31. Maximum von Mises stress in the tensile stiffener

Figures 32 to 35 show the variation of the von Mises stresses in the rectangular and triangular stiffeners with similar dimensions ( $8 \times 90 \times 100$ ) mm, in the tension and compressed zones. The stresses in the upper triangular part of the rectangular stiffener are very low. However, the stresses are almost uniform for the triangular stiffener. This allows saying that the upper triangular part of the rectangular stiffener is not efficient and can be removed to save material.

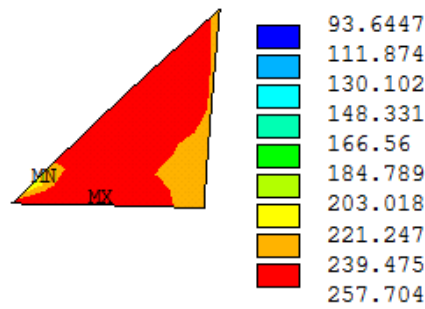


Figure 32. Von Mises stress in the triangular stiffener in tension zone (dimensions:  $8 \times 90 \times 100$  mm)

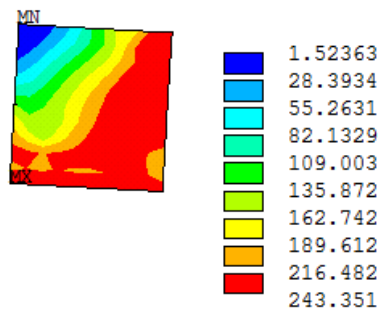


Figure 33. Von Mises stress in the rectangular stiffener in tension zone (dimensions:  $8 \times 90 \times 100$  mm)

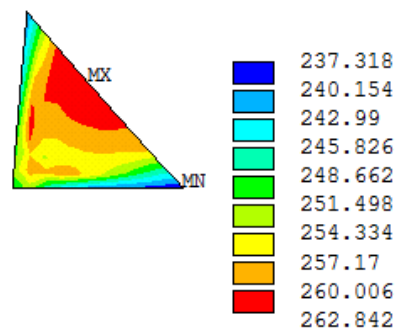


Figure 34. Von Mises stress in the triangular stiffener in compressed zone (dimensions:  $8 \times 90 \times 100$  mm)



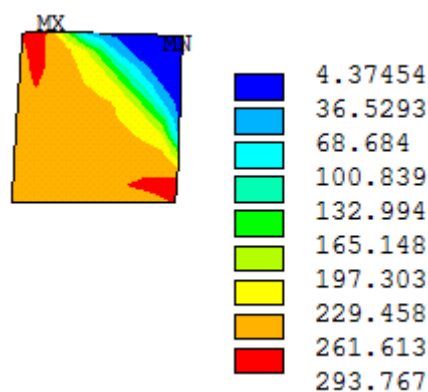


Figure 35. Von Mises stress in the rectangular stiffener in compressed zone (dimensions:  $8 \times 90 \times 100$  mm)

## 6. Conclusions

This research work aimed primarily to analyze the behaviour of a column base connection subjected to a compressive force and a bending moment. For this, a 3D numerical model was developed under the ANSYS code while considering the material nonlinearity, possible instability, and contact effect.

The results of the finite element model have been validated by the existing experimental results and compared with the analytical calculations given by the EC3 formulations considering the moment-rotation curves and the failure modes. The proposed numerical model can be considered accurate and can provide satisfactory results for the analysis of the behaviour of connections provided with stiffeners. The finite element model takes into account the different geometries and material non-linearities. Moreover, it allows representing the elasto-plastic behaviour and the instabilities of the connections, by applying a bending moment and a compressive force. The prestressing force in the anchor rods and the contact effect between the different elements are also taken into consideration.

The numerical modelling results, which have been validated against the experimental and compared with the analytical results given by the EC3, show that the proposed model can provide a lot of information about stresses and displacements of the anchor rods, the prestressing effect, and prying forces, which are usually difficult to obtain through experimental measurement.

Moreover, it was shown that the effect of each component of the connection on the stiffness and resistance of the column base depends on the combination of the applied loads (N, M). It was also observed that the anchor rods are stressed not only by normal tensile forces, as usually considered in design, but also by a local bending moment. This moment needs to be taken into consideration in the anchor rod resistance because the local moment strongly anticipates the anchor rod failure. Further, the prestressing in the anchor rods has a significant role on the initial stiffness of the column base connection.

Stiffeners have a very important impact on the stiffness and bending resistance of the column base connections. A parametric study revealed that increasing the height of the stiffeners increases the stiffness and bending resistance. In addition, it was shown that the stiffeners change the position of the compression center and reduce the prying force in the column base connection, contributing thus to improve its mechanical parameters. In addition, it was also found that the triangular stiffener is more efficient and more economical than the rectangular one. Consequently, the findings allow us to conclude that the stiffeners improve the overall performance of the column bases in stiffness and strength.

## 7. Declarations

### 7.1. Author Contributions

Conceptualization, C.B.; methodology, C.B., N.B., A.B., and A.M.; software, C.B. and N.B.; validation, C.B.; formal analysis, C.B.; investigation, C.B.; resources, C.B.; data curation, C.B.; writing—original draft preparation, C.B.; writing—review and editing, C.B., N.B., A.B., and A.M.; visualization, C.B.; supervision, N.B, A.B., and A.M.; project administration, C.B., N.B., A.B. and A.M. All authors have read and agreed to the published version of the manuscript.

### 7.2. Data Availability Statement

The data presented in this study are available in the article.

### 7.3. Funding

The authors received no financial support for the research, authorship, and/or publication of this article.

## 7.4. Conflicts of Interest

The authors declare no conflict of interest.

## 8. References

- [1] Benyelles C.M., Boumechra N., Bouchaïr A. & Missoum A., (2016). Assembly behavior of a Column Base subjected to a bending moment. Proceedings of International Seminar Innovation and Valorization in Civil Engineering Construction Materials INVACO'2016, 4th edition, Hammamet, Tunisia. (In French).
- [2] Cloete, R., & Roth, C. P. (2021). Column base connections under compression and biaxial moments: Experimental and numerical investigations. *Journal of Constructional Steel Research*, 184. doi:10.1016/j.jcsr.2021.106834.
- [3] Asif Bin Kabir, M., Sajid Hasan, A., & Muntasir Billah, A. H. M. (2021). Failure mode identification of column base plate connection using data-driven machine learning techniques. *Engineering Structures*, 240, 112389. doi:10.1016/j.engstruct.2021.112389.
- [4] Hassan, A. S., Torres-Rodas, P., Giuliotti, L., & Kanvinde, A. (2021). Strength characterization of exposed column base plates subjected to axial force and biaxial bending. *Engineering Structures*, 237. doi:10.1016/j.engstruct.2021.112165.
- [5] EN 1993-1-8. (2005). Eurocode 3: Design of steel structures-Part 1-8. European Committee for Standardization, Bruxelles, Belgium.
- [6] Shi, Y., Shi, G., & Wang, Y. (2007). Experimental and theoretical analysis of the moment-rotation behaviour of stiffened extended end-plate connections. *Journal of Constructional Steel Research*, 63(9), 1279–1293. doi:10.1016/j.jcsr.2006.11.008.
- [7] Merad Boudia, S., Benyelles, C., Boumechra, N., Missoum, A., & Bouchaïr, A. Comportement mécanique d'un tronçon en té d'assemblage boulonné avec et sans précontrainte". *Academic Journal of Civil Engineering*, 36(1), 538–541. doi:10.26168/ajce.36.1.114.
- [8] Da Silva Seco, L., Couchaux, M., Hjjaj, M., & Neves, L. C. (2021). Column base-plates under biaxial bending moment. *Engineering Structures*, 231. doi:10.1016/j.engstruct.2020.111386.
- [9] Latour, M., Piluso, V., & Rizzano, G. (2014). Rotational behaviour of column base plate connections: Experimental analysis and modelling. *Engineering Structures*, 68, 14–23. doi:10.1016/j.engstruct.2014.02.037.
- [10] Díaz, H., Nuñez, E., & Oyarzo-Vera, C. (2020). Monotonic response of exposed base plates of columns: Numerical study and a new design method. *Metals*, 10(3), 396. doi:10.3390/met10030396.
- [11] DeWolf, J. T., & Sarisley, E. F. (1980). Column Base Plates with Axial Loads and Moments. *Journal of the Structural Division*, 106(11), 2167–2184. doi:10.1061/jsdeag.0005569.
- [12] Thambiratnam, D. P., & Paramasivam, P. (1986). Base Plates Under Axial Loads and Moments. *Journal of Structural Engineering*, 112(5), 1166–1181. doi:10.1061/(asce)0733-9445(1986)112:5(1166).
- [13] Astaneh-Asl, A., & Bergsma, G. (1993). Cyclic behavior and seismic design of steel base plates. *Structural Engineering in Natural Hazards Mitigation*, 409-414, American Society of Civil Engineering (ASCE), United States.
- [14] Burda, J. J. (1999). Studies of seismic behavior of steel base plates. University of Nevada, Reno, United States.
- [15] Drake, R. M., & Elkin, S. J. (1999). Beam-column base plate design-LRFD method. *Engineering Journal-American Institute of Steel Construction*, 36, 29-38.
- [16] Gomez, I., Deierlein, G., & Kanvinde, A. (2010). Exposed column base connections subjected to axial compression and flexure. Final Report Presented to the American Institute of Steel Construction, Chicago, United States.
- [17] Wald F. (1995). Patky Sloupù, Column Base, CVUT, Praha, ISBN 80-01-01337-5, p. 137.
- [18] Wald, F., Sokol, Z., & Steenhuis, M. (1996). Proposal of the stiffness design model of the column bases. *Connections in Steel Structures III*, 249–258. doi:10.1016/b978-008042821-5/50082-1.
- [19] Steenhuis, C. M., Wald, F., Sokol, Z., & Stark, J. W. B. (2008). Concrete in compression and base plate in bending. *Heron-English Edition*, 53(1/2), 51.
- [20] Kanvinde, A. M., Grilli, D. A., & Zareian, F. (2012). Rotational Stiffness of Exposed Column Base Connections: Experiments and Analytical Models. *Journal of Structural Engineering*, 138(5), 549–560. doi:10.1061/(asce)st.1943-541x.0000495.
- [21] Picard, A., & Beaulieu, D. (1985). Behaviour of a Simple Column Base Connection. *Canadian Journal of Civil Engineering*, 12(1), 126–136. doi:10.1139/185-013.
- [22] Jaspert, J. P., & Vandegans, D. (1998). Application of the component method to column bases. *Journal of Constructional Steel Research*, 48(2–3), 89–106. doi:10.1016/S0143-974X(98)90196-1.

- [23] Hon, K. K., & Melchers, R. E. Experimental behavior of steel column bases". *Journal of Constructional Steel Research*, 9, 35–50 10.1016/0143-974X(95)00011-J.
- [24] Ermopoulos, J. C., & Stamatopoulos, G. N. (1996). Mathematical Modelling of Column Base Plate Connections. *Journal of Constructional Steel Research*, 36(2), 79–100. doi:10.1016/0143-974X(95)00011-J.
- [25] Kovács, N., Calado, L., & Dunai, L. (2004). Behaviour of bolted composite joints: Experimental study. *Journal of Constructional Steel Research*, 60(3–5), 725–738. doi:10.1016/S0143-974X(03)00139-1.
- [26] Torres-Rodas, P., Medalla, M., Zareian, F., & Lopez-Garcia, D. (2022). Cyclic behavior and design methodology of exposed base plates with extended anchor bolts. *Engineering Structures*, 260, 114235. doi:10.1016/j.engstruct.2022.114235.
- [27] Lee, D. Y., Goel, S. C., & Stojadinovic, B. (2008). Exposed column-base plate connections bending about weak axis: I. Numerical parametric study. *International Journal of Steel Structures*, 8(1), 11-27.
- [28] Delhomme, F., Debicki, G., & Chaib, Z. (2010). Experimental behaviour of anchor bolts under pullout and relaxation tests. *Construction and Building Materials*, 24(3), 266–274. doi:10.1016/j.conbuildmat.2009.08.038.
- [29] Zhao, Y., Zhang, H., & Nie, Y. (2019). Study of Shear Capacity of Jointed Rock Mass with Prestressed Anchor Bolt. *Advances in Civil Engineering*, 2019, 1–10. doi:10.1155/2019/6824543.
- [30] Razzaghi, J., & Khoshbakht, A. (2015). Numerical evaluation of column base rigidity. *International Journal of Steel Structures*, 15(1), 39–49. doi:10.1007/s13296-015-3003-7.
- [31] Falborski, T., Hassan, A. S., & Kanvinde, A. M. (2020). Column base fixity in steel moment frames: Observations from instrumented buildings. *Journal of Constructional Steel Research*, 168. doi:10.1016/j.jcsr.2020.105993.
- [32] ANSYS Inc., (2015). ANSYS 15.0 Multiphysics Utility (15<sup>th</sup> Ed.). San Jose, united States.
- [33] Benyelles C.M., Boumechra N., Bouchair A. & Missoum A. (2015). Analysis of the Behavior of the Column Base Assembly Subjected to Axial Compression. 554-562, *Proceedings of CICOMM 2015 (1<sup>st</sup> International Conference on Steel and Composite Construction*, 25-26 November, 2015, Tlemcen, Algeria. (In French).
- [34] Kumar, G., & Samanta, M. (2020). Experimental evaluation of stress concentration ratio of soft soil reinforced with stone column. *Innovative Infrastructure Solutions*, 5(1). doi:10.1007/s41062-020-0264-6.